

Hydrodynamic simulation of elliptic flow*

P.F. Kolb^{a,b}, J. Sollfrank^b, P.V. Ruuskanen^c, and U. Heinz^a

^aCERN/TH, CH-1211 Geneva 23

^bInstitut für Theoretische Physik, Universität Regensburg, D-93040 Regensburg

^cDepartment of Physics, University of Jyväskylä, FIN-40351 Jyväskylä

We use a hydrodynamic model to study the space-time evolution transverse to the beam direction in ultrarelativistic heavy-ion collisions with nonzero impact parameters. We focus on the influence of early pressure on the development of radial and elliptic flow. We show that at high energies elliptic flow is generated only during the initial stages of the expansion while radial flow continues to grow until freeze-out. Quantitative comparisons with SPS data from semiperipheral Pb+Pb collisions suggest the applicability of hydrodynamical concepts already ≈ 1 fm/c after impact.

1. Hydrodynamic model with longitudinal boost invariance

The transverse expansion dynamics in non-central heavy-ion collisions at SPS energies has recently attracted much attention [1–7]. We here study it within the hydrodynamic model. In order to reduce the complexity of the numerical task we follow [4] and implement analytically Bjorken scaling flow with $v_z = z/t$ in the longitudinal direction and only solve the transverse dynamics numerically. The Bjorken ansatz holds exactly at infinite beam energy, but properly restricted to a finite rapidity interval it is phenomenologically successful also at SPS and AGS energies [8]. It breaks down, however, near target and projectile rapidities; using it we can therefore reliably compute the transverse expansion only near midrapidity.

The system of hydrodynamic equations is closed by an equation of state (EOS) $p(e, n)$ giving the pressure as a function of energy and baryon density. Hydrodynamics thus provides a direct relation between the EOS and the dynamical evolution of the system. To study the dynamical effects of a softening of the EOS in the neighborhood of a phase transition to quark-gluon plasma we use three different equations of state. EOS I is the hard equation of an ideal ultrarelativistic gas, $p = e/3$. EOS H is the much softer EOS for a gas of interacting hadron resonances; for $n \approx 0$ it satisfies $p \approx 0.15 e$. A Maxwell construction between these two EOS, adding a bag pressure $B^{1/4} = 230$ MeV, results in EOS Q which has a phase transition at $T_{\text{cr}}(n = 0) = 164$ MeV with a latent heat of 1.15 GeV/fm³ [9]. The system is frozen out at a fixed decoupling temperature T_{dec} , and all unstable resonances are allowed to decay before we compare with experimental data.

*This work was supported by BMBF, DFG and GSI.

2. Space time evolution of the reaction zone

We initialize the reaction zone with transverse energy and baryon density profiles which are taken to be proportional to the transverse density of wounded nucleons calculated from the Glauber model [4,10]. The initial configuration is thus parametrized by the equilibration time τ_0 and the maximum energy and baryon densities e_0 and n_0 in central

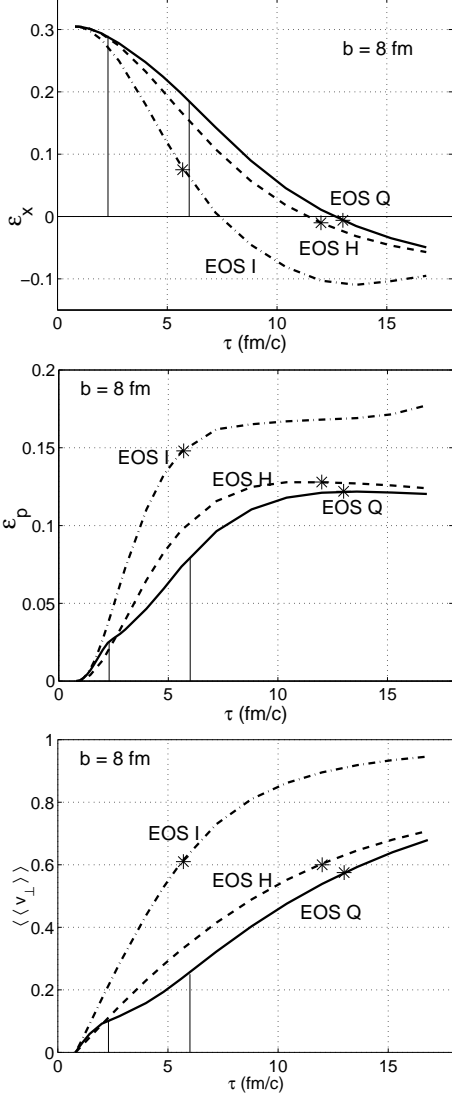


Figure 1. Time evolution of the spatial eccentricity ϵ_x (top), the momentum anisotropy ϵ_p (middle), and the radial flow $\langle\langle v_{\perp} \rangle\rangle$ (bottom).

Fig. 1 was computed for 158 A GeV Pb+Pb collisions at $b = 8$ fm. For EOS Q the vertical lines indicate when the center of the reaction zone goes from plasma to mixed phase and from mixed to hadron phase, respectively. One sees that 1/6 of the final elliptic flow is generated before the pure QGP phase disappears, 1/2 in the mixed phase, and about 1/3 in the hadronic phase. The stars indicate the freeze-out point ($T_{\text{dec}} = 120$ MeV).

collisions. For each EOS these parameters and the decoupling temperature are fixed by a fit [10] to the negative hadron and net proton m_t -spectra at midrapidity from central Pb + Pb collisions at 158 AGeV [11]. The spectra for non-central collisions are then predicted without extra parameters.

The hydrodynamic evolution provides the time-dependence of the matter in coordinate and momentum space. In non-central collisions, the initial spatial deformation of the reaction zone in the transverse plane, characterized by its spatial eccentricity $\epsilon_x = \frac{\langle\langle y^2 - x^2 \rangle\rangle}{\langle\langle y^2 + x^2 \rangle\rangle}$, leads to anisotropic pressure gradients and a preferred buildup of transverse flow in the shorter x -direction [4]. (x lies inside, y points orthogonal to the collision plane. $\langle\langle \dots \rangle\rangle$ denotes the energy density weighted spatial average at fixed time.) This leads to a growing flow anisotropy, characterized by $\epsilon_p = \frac{\langle\langle T^{xx} - T^{yy} \rangle\rangle}{\langle\langle T^{xx} + T^{yy} \rangle\rangle}$. At freeze-out this hydrodynamic quantity is directly related to the elliptic flow $v_2 = \langle \cos(2\varphi) \rangle$, defined by an average over the final particle momentum spectrum; for pions $\epsilon_p \approx 2v_2$ [7]. In contrast to v_2 , ϵ_p can be studied as a function of time and gives access to the buildup of elliptic flow.

The developing stronger flow into the collision plane leads to a decrease of ϵ_x with time; the buildup of elliptic flow thus slows down and eventually *shuts itself off*. This is clearly seen in the upper two panels of Fig. 1: ϵ_p saturates when ϵ_x passes through zero. For a hard EOS this happens faster than for a soft one; also, the total amount of elliptic flow which can be generated by a given EOS increases with its hardness $c_s^2 = \frac{\partial e}{\partial p}$.

For EOS I the system freezes out before the elliptic flow is fully developed; for EOS H and EOS Q the opposite is true. The radial flow, characterized by $\langle\langle v_{\perp} \rangle\rangle = \langle\langle \gamma \sqrt{v_x^2 + v_y^2} \rangle\rangle / \langle\langle \gamma \rangle\rangle$ (where γ is the Lorentz factor), does not saturate: Fig. 1 shows that it continues to grow monotonously until freeze-out, even after the elliptic flow has saturated, due to the continued presence of *essentially azimuthally symmetric* radial pressure gradients.

Note the important role of the EOS: a softer EOS, especially its softening near a phase transition, delays the buildup of both radial and elliptic flow. It also reduces the maximally achievable value of the latter. At low energies, freeze-out (driven by cooling and expansion due to radial flow) happens before the elliptic flow has fully developed. To achieve fully developed elliptic flow lower beam energies are required for softer equations of state [7,10]. This reflects both the lower saturation value of ϵ_p for the softer EOS and the slower buildup of radial flow, resulting in more available time until freeze-out.

3. Transverse mass spectra and applicability of hydrodynamics

Collective flow affects the measurable momentum spectra of the produced particles. We showed in [7] that our model is able to describe the measured asymmetries of the particle spectra; the calculated elliptic flow $v_2 = \langle \cos(2\varphi) \rangle$ at midrapidity agrees well with the published data [1]. Here we discuss the impact parameter dependence of the azimuthally

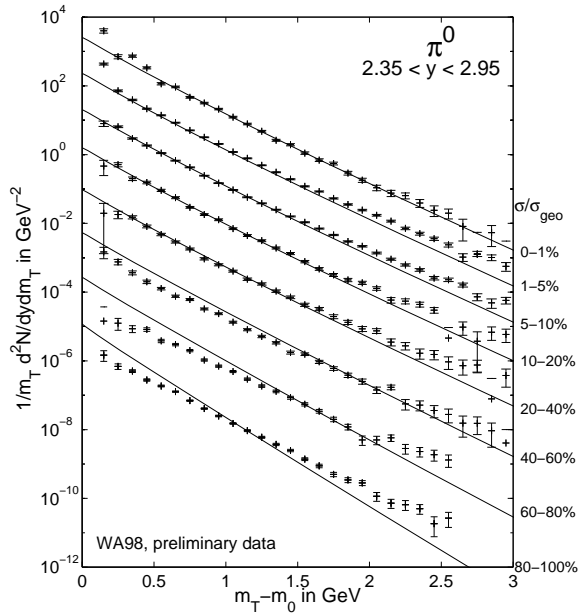


Figure 2. Preliminary π^0 transverse mass spectra from Pb+Pb collisions of varying centrality measured by WA98 [2]. The lines show our hydro results.

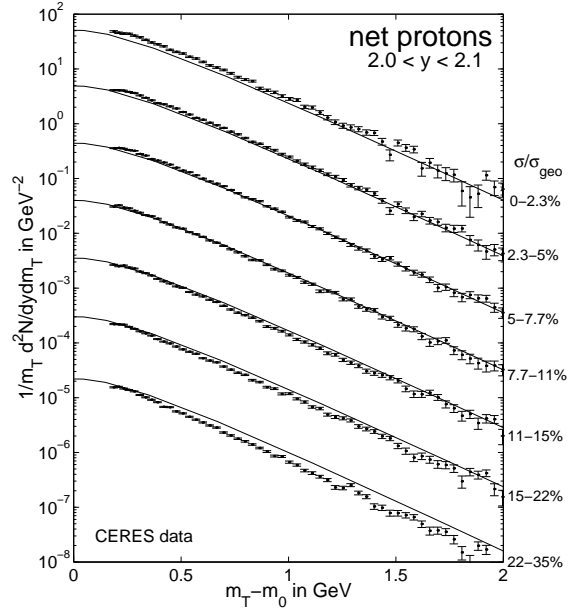


Figure 3. Same as Fig. 2, but for net protons measured by the CERES Collaboration [3]. Note the different impact parameter binning in Figs. 2 and 3.

integrated transverse mass spectra and show that, once tuned to central collision data, hydrodynamics successfully reproduces the magnitude and shape of the spectra up to impact parameters of about 8-10 fm. Figs. 2 and 3 show preliminary data on transverse mass spectra of neutral pions (WA98 Collaboration [2]) and net protons (CERES Collaboration [3]) from 158 A GeV Pb+Pb collisions of varying centrality. The lines indicate

our hydrodynamical results at midrapidity, obtained with EOS Q and initial conditions tuned to central collisions as described above. The WA98 data extend to very peripheral collisions: the lowest spectrum in Fig. 2 corresponds to $b=13$ fm where hydrodynamics certainly loses its applicability. At such large impact parameters one does not observe the collision of two nuclei, but rather two dilute nucleon clouds penetrating each other. At smaller impact parameters the model fails in the high- m_t region; here hard scattering processes begin to dominate which cannot be modeled hydrodynamically. Up to $b \approx 10$ fm (bin 6 represents impact parameters up to 11 fm [2]) and transverse masses of about 2 GeV, however, hydrodynamics works very well, both for the pion and net proton spectra. (For the latter the CERES data in Fig. 3 do not extend to very peripheral collisions, the largest measured impact parameters corresponding to about 8.4 fm [3].)

4. Summary

We have demonstrated the interplay between spatial eccentricity as the driving force for generating momentum space asymmetries and the back-reaction of the latter on the former. Comparison with measured spectra from Pb+Pb collisions with varying impact parameter showed that the hydrodynamical model successfully reproduces the data up to $b=8-10$ fm. The good quantitative agreement between data and model suggests rather rapid thermalization in the reaction zone. If final data confirm that the elliptic flow is essentially saturated in Pb+Pb collisions at the SPS, this would provide strong evidence for very early pressure in the system. In our calculations a large fraction of the finally observed elliptic flow is generated while the energy density exceeds the critical value $e_{\text{cr}} = 1$ GeV/fm³ for deconfinement. This confirms the suggestion [5] that elliptic flow is a probe for the *early collision stage*.

We thank Th. Peitzmann (WA98) and F. Ceretto (CERES) for sending us their preliminary data prior to publication. P.K. wishes to express his gratitude to the CERN Summer Student Programme and thanks T. Peeter's group for their warm hospitality.

REFERENCES

1. H. Appelshäuser et al. (NA49 Coll.), Phys. Rev. Lett. 80 (1998) 4136
2. C. Blume, PhD thesis, Universität Münster, 1998; M.M. Aggarwal et al. (WA98 Collaboration), Phys. Rev. Lett 81 (1998) 4087
3. F. Ceretto, PhD Thesis, Universität Heidelberg, 1998; P. Braun-Munzinger, J. Stachel, Nucl. Phys. A 638 (1998) 3c
4. J.Y. Ollitrault, Phys. Rev. D 46 (1992) 229
5. H. Sorge, Phys. Lett. B 402 (1997) 251; Phys. Rev. Lett. 82 (1999) 2048
6. D. Teaney, E. Shuryak, nucl-th/9904006
7. P.F. Kolb, J. Sollfrank, U. Heinz, nucl-th/9906003, Phys. Lett. B, in press
8. H. Dobler, J. Sollfrank, U. Heinz, nucl-th/9904018, Phys. Lett. B, in press
9. J. Sollfrank et al., Phys. Rev. C 55 (1997) 392
10. P.F. Kolb, Diploma Thesis, Universität Regensburg, 1999; P.F. Kolb, J. Sollfrank, U. Heinz, in preparation
11. H. Appelshäuser et al. (NA49 Coll.), Phys. Rev. Lett. 82 (1999) 2471